How to cite: *Angew. Chem. Int. Ed.* **2021**, *60*, 19058–19062
International Edition: doi.org/10.1002/anie.202106517
German Edition: doi.org/10.1002/ange.202106517

RNA Modification Hot Paper

RNA-Cleaving Deoxyribozymes Differentiate Methylated Cytidine Isomers in RNA

*Anam Liaqat[+], Maksim V. Sednev[+], Carina Stiller, and Claudia Höbartner**

In memory of Professor Siegfried Hünig

Abstract: *Deoxyribozymes are emerging as modification-specific endonucleases for the analysis of epigenetic RNA modifications. Here, we report RNA-cleaving deoxyribozymes that differentially respond to the presence of natural methylated cytidines, 3-methylcytidine (m^3C), N^4-methylcytidine (m^4C), and 5-methylcytidine (m^5C), respectively. Using in vitro selection, we found several DNA catalysts, which are selectively activated by only one of the three cytidine isomers, and display 10- to 30-fold accelerated cleavage of their target m^3C-, m^4C- or m^5C-modified RNA. An additional deoxyribozyme is strongly inhibited by any of the three methylcytidines, but effectively cleaves unmodified RNA. The m^XC-detecting deoxyribozymes are programmable for the interrogation of natural RNAs of interest, as demonstrated for human mitochondrial tRNAs containing known m^3C and m^5C sites. The results underline the potential of synthetic functional DNA to shape highly selective active sites.*

Posttranscriptional nucleotide modifications are indispensable for the functional diversity of cellular RNA. More than 170 types of modified nucleotides are known,[1] but detection and quantification remain challenging. Transcriptome-wide maps are available for some modifications,[2] but the predicted sites and derivatization levels must be further validated by alternative methods.[3] Recently, we reported RNA-cleaving deoxyribozymes that reliably report the presence of N^6-alkyladenosines.[4] Deoxyribozymes responsive to N^6-methyladenosine (m^6A) have been used to interrogate m^6A levels in lncRNA, snoRNA and mRNA in DGACH sequence motifs,[4a,5] and the results were in agreement with those obtained by the current benchmark in the field (the SCARLET assay).[6] We found that DNA enzymes activated by m^6A reached 5–10-fold faster cleavage rates for modified vs. unmodified substrate.[4a] The bulkier and more hydrophobic N^6-isopentenyladenosine (i^6A) in the RNA had a much stronger activating effect on deoxyribozyme-catalyzed RNA cleavage, leading up to 2500-fold faster cleavage of the i^6A-modified versus unmodified RNA substrate.[4b]

The finding of m^6A- and i^6A-sensitive deoxyribozymes inspired the search for DNA catalysts that target other RNA modifications. Deoxyribozymes that are able to differentiate the three natural monomethylated cytidine isomers 3-methylcytidine (m^3C), N^4-methylcytidine (m^4C) and 5-methylcytidine (m^5C), and distinguish them from unmodified cytidine, are of particular interest. These methylated cytidines exhibit different structural properties depending on the location of the methyl group (Figure 1a). The methyl group in m^3C disrupts Watson–Crick base pairing and confers a positive charge to the nucleobase.[7] As a result, m^3C may promote the formation of alternative secondary structures. Similarly to m^6A, the methyl group in m^4C is attached to the exocyclic amino group, and depending on its conformation, m^4C can either retain (in *anti*-conformation) or disrupt Watson–Crick base pairing (in *syn*-conformation).[8] The *anti*-conformation is enforced in a base-paired structure but destabilized by steric repulsion (Figure 1a). In contrast to m^4C, the methyl group in m^5C does not disturb base pairing directly but may

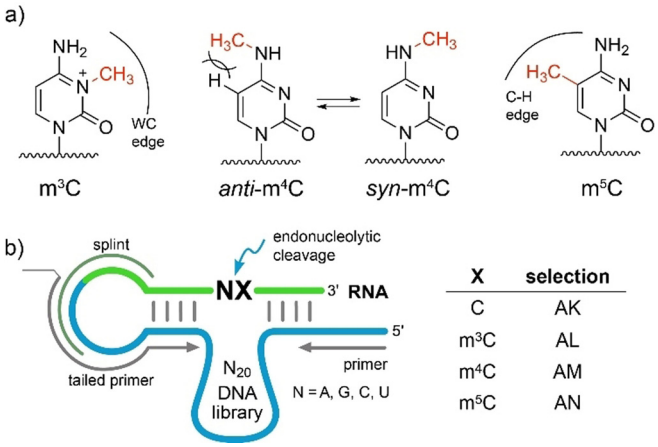

Figure 1. a) Structures of three natural methylated cytidines and their structural consequences. m^3C blocks the Watson–Crick (WC) edge and confers a positive charge to the nucleobase. m^4C retains WC base pairing in *anti*-conformation which is destabilized by steric clash between 5-H and N^4-Me. In *syn*-conformation, m^4C hinders WC base pairing. m^5C enhances hydrophobicity in the major groove and improves base stacking. b) Design of in vitro selection libraries. Splint for ligation and primer binding sites are indicated. Detailed selection is shown in Figure S1.

[*] A. Liaqat,[+] Dr. M. V. Sednev,[+] C. Stiller, Prof. Dr. C. Höbartner
Institute of Organic Chemistry, University of Würzburg
Am Hubland, 97074 Würzburg (Germany)
E-mail: claudia.hoebartner@uni-wuerzburg.de
[+] These authors contributed equally to this work.
Supporting information and the ORCID identification number(s) for the author(s) of this article can be found under: https://doi.org/10.1002/anie.202106517.

interact with neighboring nucleotides via the C–H-edge. The m^5C modification is known to enhance base stacking.[9] Targeting these methylated cytidine isomers also addresses fundamental questions on scope and plasticity of DNA catalysis.

To identify modification-specific catalysts, we performed gel-based in vitro selection experiments[4] (arbitrarily named AL, AM and AN, Figure 1b) using an N_{20} DNA library and three synthetic RNA substrates, each containing one of the three monomethylated cytidines (R2-R4, Table S1). Negative selection rounds were carried out with unmodified RNA (R1) to enhance the selectivity for the modified RNA. In this way, DNA enzymes that can cleave both unmodified and modified RNA were eliminated (Figure S1). In parallel, we sought DNA enzymes that preferentially cleave unmodified RNA and are inhibited by m^xC (AK selection). In this case, the positive selection was performed with R1 and the negative selection used an equimolar mixture of R2-R4. To evolve potentially universal DNA catalysts that respond to the cytidine modifications within all four possible dinucleotide sequence motifs NC, the RNA substrates contained a degenerate nucleotide upstream of the target cytidine.

After 18 rounds of selection, the enriched DNA pools were cloned, and 10 clones of each selection were sequenced. We identified 36 unique sequences (D6-D41, Table S2), suggesting a high diversity in the selection libraries. To obtain further insights into the library composition and to potentially identify further DNAzyme candidates, we applied next-generation sequencing (NGS) for a deeper analysis of AK, AL, AM and AN selection pools. In total, eight libraries were sequenced, including rounds 7 and 18 from each of the four in vitro selections. Deoxyribozymes specific for m^3C, m^4C or m^5C should be enriched in selection libraries AL, AM or AN, respectively, and depleted in selection AK. Conversely, the deoxyribozymes inhibited by a modification would be highly enriched in selection AK and depleted in selections AL, AM or AN. In this way, using $\log_2$ fold change in abundance ($\log_2 f_{CA}$) between selection rounds 7 and 18 we identified nine additional candidate DNA sequences (D42-D50, Table S2).[10]

Overall, 45 DNA sequences were then tested individually for their ability to cleave sixteen 3′-fluorescently labeled RNA substrates R5-R20 in independent cleavage reactions. The degenerate position was substituted with one of the four canonical ribonucleotides. Together R5-R20 represented every possible combination of four different junctions and four cytidine variants. After removing the 5′-overhang and 3′-loop region, 28 deoxyribozymes retained trans-cleaving activity (Table S3).

Using RNase T1 digestion and alkaline hydrolysis ladders, we determined the cleavage site for every active DNA enzyme. In accordance with the initial design, all tested deoxyribozymes cleaved the RNA substrate near the target cytidine (Table S3). The activity data partially supported our hypothesis that differences in enrichment in the selection libraries correlate with the specificity of deoxyribozymes. The correlation was good for DNAzymes found in the AK, AL and AM selections. However, poor correlation was observed for the selection AN, as the majority of the AN DNA enzyme candidates cleaved both m^5C-modified and unmodified RNA nearly to the same extent despite large differences in fold change abundance values (Table S3).

Interestingly, the inspection of predicted secondary structures revealed that none of the active deoxyribozymes contained the 8–17 motif, which had been repeatedly found in independent in vitro selections of RNA-cleaving deoxyribozymes.[4a,11] Its absence is especially surprising for AK selection, which used unmodified RNA as substrate. Probably, the 8–17 variants, that were initially present in the selection pools, were not particularly selective for either modified or unmodified RNA, and therefore were depleted during negative selection rounds. None of previously reported 8–17 variants was particularly efficient at cleaving N|C junctions.[11]

With respect to the degenerate position in the RNA substrate that was introduced to evolve for sequence generality, only deoxyribozyme AL112 distinguished a cytidine modification almost equally well in all four NC sequence contexts. On the other hand, many DNA catalysts were good at differentiating methylated from unmethylated RNA in one or two sequence contexts. In fact, we identified a corresponding deoxyribozyme for almost every combination of modification and junction (Table S3). For the UC junction in particular, we found that AL112, AM101, AN05 and AK104 (Figure 2a) deoxyribozymes together achieved efficient differentiation for all three monomethylated cytidines. Among these, AL112, AM101 and AN05 preferentially cleaved Um^3C-, Um^4C- and Um^5C-containing RNAs, respectively (fraction cleaved (FC) for the corresponding modified RNA $FC_{UmXC} \geq 70\,\%$, and unmodified RNA $FC_{UC} \leq 30\,\%$ after 6 h, see Figure 2b and Table S3), while AK104 efficiently cleaved only the UC substrate and was inhibited by all the modified nucleotides ($FC_{UC} = 85\,\%$, $FC_{UmXC} \approx 0$ after 6 h). Therefore, this set of deoxyribozymes was further characterized.

First, we confirmed the cleavage sites determined by the gel-based assay (Figure S3) by mass spectrometry. Consistent with the general mechanism proposed for DNA-catalyzed RNA cleavage,[12] the cleavage products for all four selected catalysts contained 2′,3′-cyclic phosphate and 5′-OH termini (Figure S4).

Deoxyribozyme AL112 preferentially cleaved m^3C-modified RNA in all four NC sequence contexts with the highest cleavage yield for the UC junction ($FC_{Um3C} = 70\,\%$, Figure S5). In the UC context, AL112 showed a ca. 30-fold higher k_{obs} value for m^3C-RNA compared to unmodified RNA (Figure 2b). The cleavage site was situated directly upstream of the modified nucleotide m^3C. Analysis of the predicted secondary structure showed that presence of m^3C might be required for disruption of the dG1-rC16 base pair that otherwise inhibited RNA cleavage for the NC-, Nm^4C- and Nm^5C-RNA substrates (Figure 2b, Table S3).

Deoxyribozyme AM101 was specific for m^4C and cleaved Um^4C-RNA ca. 10 times faster than UC-RNA. The cleavage site of AM101 was one nucleotide downstream of the modification site. Analysis of the secondary structure revealed the presence of a dG18-rU15 wobble base pair, which might be responsible for selectivity of AM101 for the UC junction (Figure 2a). However, in the CC sequence

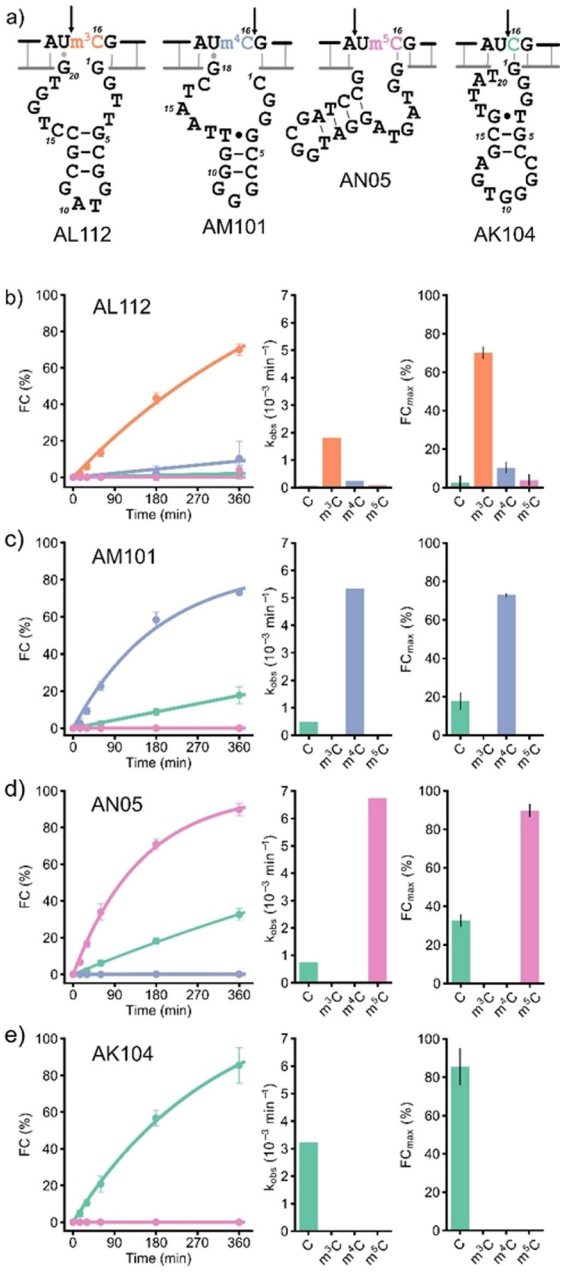

Figure 2. a) Sequences and predicted secondary structures of selected deoxyribozymes found in this study. The arrow indicates the cleavage site. Kinetic characterization of b) AL112, c) AM101, d) AN05, e) AK104 with four RNA substrates R8 (UC), R12 (Um^{3}C), R16 (Um^{4}C) and R20 (Um^{5}C). b)—e): Single-turnover kinetics plots (left). Observed rate constants k_{obs} (middle). Cleavage yields FC_{max} after 6 h incubation (right: mean of three independent experiments with error bars showing SD); representative gel images are in the supporting information). Reaction conditions: 1 μM RNA, 10 μM deoxyribozyme, 20 mM $MgCl_2$, 50 mM Tris-HCl, 150 mM NaCl, pH 7.5, 37 °C.

context, where formation of the stronger Watson–Crick base pair dG18-rC15 is expected, a significant decrease in cleavage activity was observed (Figure S6, Table S3). Interestingly, AM101 also discriminated against N^4,N^4-dimethylcytidine (m^{4,4}C), which was cleaved at nearly the same rate as unmodified RNA (Figure S7).

The deoxyribozyme AN05 for cleavage of m^{5}C-modified RNA was found in Sanger sequencing data of the AN selection. Analysis of NGS data showed that it was also present in the AK selection, where it was strongly depleted from round 7 to round 18 (Table S3). In the UC context, AN05 cleaved only m^{5}C-modified and unmodified substrates ($FC_{Um^5C} = 90\,\%$, $FC_{UC} = 33\,\%$), and was completely inhibited by m^{3}C and m^{4}C. The kinetic discrimination ability of AN05 was comparable to AM101: AN05 cleaved Um^{5}C-RNA ca. 10 times faster than the corresponding unmodified substrate (Figure 2b, S8, and Table S3). The cleavage site of AN05 was located one nucleotide upstream of the target cytosine. The predicted secondary structure contained the dG1-rC16 base pair that might stabilize an active site which is responsible for preference of AN05 to m^{5}C and C (Figure 2a). In case of m^{3}C and m^{4}C, this base pair might be destabilized or disrupted and thus lead to inhibition of cleavage.

The recognition of m^{5}C by AN05 raised the question about the oxidized variants 5-hydroxymethylcytosin (hm^{5}C) and 5-formylcytosin (f^{5}C), previously reported in RNA as products of TET2 and ALKBH1 enzymes.[13] AN05 cleaved hm^{5}C-containing RNA slightly slower but to a similar extent as m^{5}C RNA, while f^{5}C was comparable to unmodified RNA (Figure S9). Surprisingly, this result is in line with bisulfite sequencing, which is unable to distinguish m^{5}C from hm^{5}C, and f^{5}C from C.[14] Given the functional importance of hm^{5}C and f^{5}C in natural RNA,[13] future in vitro selection experiments may be directed to evolve deoxyribozymes specific for the individual oxidized m^{5}C variants.

Deoxyribozyme AK104 efficiently cleaved unmodified RNA (FC ≥ 85 % after 6 h) and was inhibited by all cytosine modifications in AC, GC and UC sequence contexts. In this case, the cleavage site was situated directly upstream of the target cytosine. However, when the RNA substrates with the CC junction were used, AK104 cleaved the m^{3}C-containing RNA with a moderate yield (FC_{Cm^3C} ca. 30 %) and was inactive with the unmodified substrate. The cleavage site for the Cm^{3}C-RNA was shifted one nucleotide upstream (Figure S10, Table S3). This odd behavior can be explained by disruption of the dG1-rC16 base pair by m^{3}C in Am^{3}C-, Gm^{3}C- and Um^{3}C-RNAs and formation of an alternative GC base pair between dG1 and rC15 in case of Cm^{3}C-RNA. The new base pair leads to repositioning of the AK104 active site and partial rescue of the cleavage activity. On the other hand, both rC15 and rC16 in the CC-substrate can form base pairs with dG2 and dG1, respectively, thereby disrupting the functional active site and abolish the catalytic activity of AK104. Thus, AK104 is a RNA-cleaving DNA enzyme for DC junctions (D = A,G,U), with high selectivity for unmodified RNA even under accelerated cleavage conditions at elevated Mg^{2+} concentrations. None of the modified RNAs was cleaved, and RNAs with rC16 changed to U, G, or A were also not cleaved (Figures S11, S12, S13).

Next, we examined the deoxyribozymes in the more challenging situation when all three RNA isomers (Um^{3}C-, Um^{4}C- and Um^{5}C-RNAs) are present at the same time. For this experiment, we labeled the three methylated UC-RNA substrates (R12, R16 and R20) at the 2′-OH of rA9 with fluorescent N^6-(6-aminohexyl)-ATP derivatives, carrying

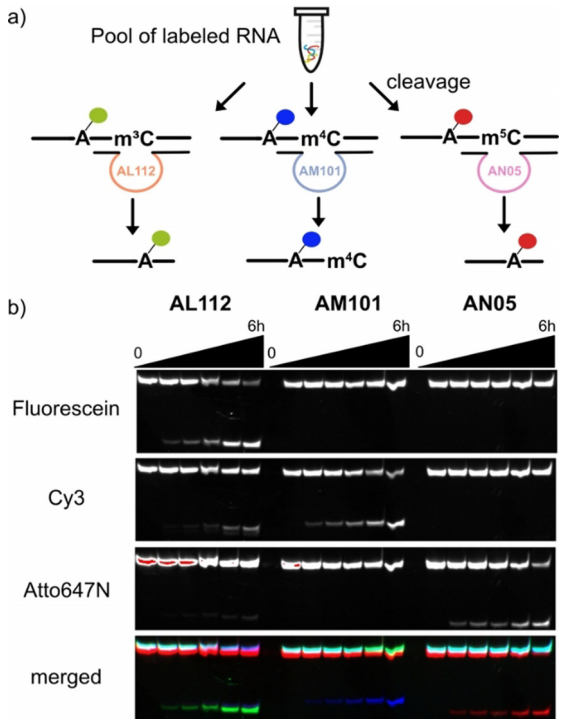

Figure 3. a) Schematic representation of selective RNA cleavage with AL112, AM101 and AN05. RNA substrates R12, R16 and R20 were separately labeled with 6FAM, Cy3 and Atto647N, respectively,[15] pooled and the mixture was subjected to cleavage with each of the three modification-specific DNAzymes. b) PAGE analysis of the experiment. Individual imaging channels for the three fluorophores are shown in black and white, and the merged image in false-color representation. Reaction conditions: 1 μM RNA mixture, 10 μM deoxyribozyme, 20 mM $MgCl_2$, 50 mM Tris-HCl, 150 mM NaCl, 37 °C.

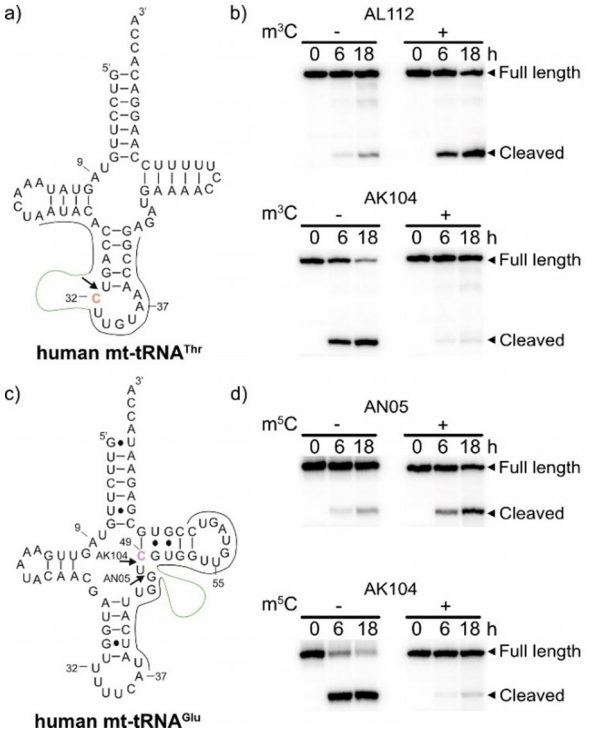

Figure 4. a) Secondary structure of mt-tRNA^{Thr} with target C32 in orange. b) PAGE analysis of mt-tRNA^{Thr} cleaved with AL112 and AK104. c) Secondary structure of mt-tRNA^{Glu} with target C49 in violet. d) PAGE analysis of mt-tRNA^{Glu} cleaved with AN05 and AK104. The cleavage reactions were performed at 37 °C. The arrows indicate the cleavage sites. Binding sites for DNAzymes are shown (binding arms in gray, catalytic core in green).

6FAM, Cy3 and ATTO-647N, respectively.[15] An equimolar mixture of the three labeled RNAs was then incubated with 10-fold excess of the AL112, AM101 or AN05 deoxyribozyme, respectively (Figure 3a). The cleavage reactions were analyzed by denaturing PAGE and imaged using a dedicated channel for each fluorescent label (Figure 3b). As expected, AL112 showed preferential cleavage of Um^{3}C-RNA with negligible signals in the m^{4}C- and m^{5}C-channels. At the same time, AM101 and AN05 cleaved only their cognate substrates with no detectable cleavage products in other channels. The results demonstrated that the specificity of each DNAzyme for its target modification was retained, and this collection of deoxyribozymes can be used to examine the identity of methylated cytidines in UC motifs. In this regard, m^{4}C-specific RNA cleavage is particularly important, as in contrast to m^{3}C and m^{5}C, there are no specific chemical reactions reported for the detection of m^{4}C in RNA.[16]

Next, we tested deoxyribozymes AL112, AN05 and AK104 on longer RNA substrates with complex secondary structures. To this end, we chose human mt-tRNA^{Thr}, which contains a known m^{3}C in the anticodon loop (C32, Figure 4a),[17] and mt-tRNA^{Glu} with a known m^{5}C at C49 (Figure 4c).[17] The single-modified tRNAs were assembled from synthetic RNA fragments by splinted ligation with T4 RNA ligase, and the binding arms of deoxyribozymes were designed to cleave the tRNAs upstream of the corresponding modification sites.[18] The results of the cleavage reactions for unmodified and modified tRNAs were compared (Figure 4b,d). AK104 cleaved both unmodified tRNAs with a high yield (>90% after 18 h) and was nearly completely inhibited by m^{3}C and by m^{5}C. AL112 and AN05 cleaved m^{3}C-modified mt-tRNA^{Thr} and m^{5}C-modified mt-tRNA^{Glu}, respectively, both somewhat less efficiently than their cognate substrates R12 and R20 (58% and 42% after 18 h), but the unmodified tRNAs did not undergo any significant cleavage. Therefore, AL112 and AN05 can faithfully identify m^{3}C- and m^{5}C-modified tRNA, respectively.

In summary, we have identified and characterized a series of RNA-cleaving deoxyribozymes that differentially respond to the presence of methylated cytidines in RNA. On the one hand, the methyl groups in m^{3}C, m^{4}C and m^{5}C can dramatically inhibit deoxyribozyme-catalyzed RNA cleavage (as in case of AK104). On the other hand, the presence of methylcytidines can lead to accelerated cleavage of modified RNA (as in case of AL112, AM101 and AN05). Owing to these kinetic differences, new deoxyribozymes can be used to examine the identity of methylcytidines and the degree of their methylation at selected target sites. The effect of the methyl group on catalytic activity might be related to steric, electrostatic (m^{3}C) or hydrophobic interaction of the modified nucleotide with its neighbors and Mg^{2+} in the active site.

The detailed structural basis for the selective recognition of methylcytidines remains to be identified.

As the enriched libraries for selection of methylcytidine-sensitive deoxyribozymes remained highly diverse even after 18 rounds of selection, we expect that many DNA enzymes with potentially interesting properties remained undiscovered. To this end, massively parallel activity assays that are able to screen cleavage reactions of thousands of candidate deoxyribozymes are required. Given the recent success in using deep sequencing for large-scale characterization of (deoxy)ribozyme kinetics,[19] new catalytic DNA motifs can likely be revealed in the future. The related experiments are currently ongoing in our laboratory and expected to uncover hidden treasures in in vitro selection libraries.

Acknowledgements

This work was supported by the DFG (SPP1784) and by the ERC (grant no. 682586). A.L. acknowledges funding by a PhD scholarship from the German Academic Exchange Service (DAAD). M.V.S. thanks the Graduate School of Life Sciences at the University of Würzburg for a Postdoc Plus fellowship. Illumina sequencing was performed at the Core Unit Systems Medicine at the University of Würzburg. Open access funding was enabled and organized by Projekt DEAL.

Conflict of Interest

The authors declare no conflict of interest.

Keywords: deoxyribozymes · epitranscriptomics · in vitro selection · RNA modification · site-specific RNA cleavage

[1] a) P. Boccaletto, M. A. Machnicka, E. Purta, P. Piątkowski, B. Bagiński, T. K. Wirecki, V. de Crécy-Lagard, R. Ross, P. A. Limbach, A. Kotter, M. Helm, J. M. Bujnicki, *Nucleic Acids Res.* **2018**, *46*, D303 – D307; b) P. J. McCown, A. Ruszkowska, C. N. Kunkler, K. Breger, J. P. Hulewicz, M. C. Wang, N. A. Springer, J. A. Brown, *Wiley Interdiscip. Rev. RNA* **2020**, *11*, e1595.

[2] J.-J. Xuan, W.-J. Sun, P.-H. Lin, K.-R. Zhou, S. Liu, L.-L. Zheng, L.-H. Qu, J.-H. Yang, *Nucleic Acids Res.* **2018**, *46*, D327 – D334.

[3] a) M. Helm, Y. Motorin, *Nat. Rev. Genet.* **2017**, *18*, 275 – 291; b) B. Linder, S. R. Jaffrey, *Cold Spring Harbor Perspect. Biol.* **2019**, *11*, a032201.

[4] a) M. V. Sednev, V. Mykhailiuk, P. Choudhury, J. Halang, K. E. Sloan, M. T. Bohnsack, C. Höbartner, *Angew. Chem. Int. Ed.* **2018**, *57*, 15117 – 15121; *Angew. Chem.* **2018**, *130*, 15337 – 15341; b) A. Liaqat, C. Stiller, M. Michel, M. V. Sednev, C. Höbartner, *Angew. Chem. Int. Ed.* **2020**, *59*, 18627 – 18631; *Angew. Chem.* **2020**, *132*, 18786 – 18790; c) R. Micura, C. Höbartner, *Chem. Soc. Rev.* **2020**, *49*, 7331 – 7353.

[5] M. Bujnowska, J. Zhang, Q. Dai, E. M. Heideman, J. Fei, *J. Biol. Chem.* **2020**, *295*, 6992 – 7000.

[6] N. Liu, M. Parisien, Q. Dai, G. Zheng, C. He, T. Pan, *RNA* **2013**, *19*, 1848 – 1856.

[7] a) L. Flemmich, S. Heel, S. Moreno, K. Breuker, R. Micura, *Nat. Commun.* **2021**, *12*, 3877; b) S. Mao, P. Haruehanroengra, S. V. Ranganathan, F. Shen, T. J. Begley, J. Sheng, *ACS Chem. Biol.* **2021**, *16*, 76 – 85.

[8] a) R. Micura, W. Pils, C. Höbartner, K. Grubmayr, M. O. Ebert, B. Jaun, *Nucleic Acids Res.* **2001**, *29*, 3997 – 4005; b) S. Mao, B. Sekula, M. Ruszkowski, S. V. Ranganathan, P. Haruehanroengra, Y. Wu, F. Shen, J. Sheng, *Nucleic Acids Res.* **2020**, *48*, 10087 – 10100.

[9] a) L. Trixl, A. Lusser, *Wiley Interdiscip. Rev. RNA* **2019**, *10*, e1510; b) E. M. Harcourt, A. M. Kietrys, E. T. Kool, *Nature* **2017**, *541*, 339 – 346; c) S. Wang, E. T. Kool, *Biochemistry* **1995**, *34*, 4125 – 4132.

[10] We picked the candidates with the largest differences between $\log_2 f_{CA}$ and $\log_2 f_{CA,neg}$ (see Table S3).

[11] a) S. W. Santoro, G. F. Joyce, *Proc. Natl. Acad. Sci. USA* **1997**, *94*, 4262 – 4266; b) J. Li, W. Zheng, A. H. Kwon, Y. Lu, *Nucleic Acids Res.* **2000**, *28*, 481 – 488; c) R. P. G. Cruz, J. B. Withers, Y. Li, *Chem. Biol.* **2004**, *11*, 57 – 67; d) K. Schlosser, Y. Li, *Biochemistry* **2004**, *43*, 9695 – 9707; e) J. C. F. Lam, J. B. Withers, Y. Li, *J. Mol. Biol.* **2010**, *400*, 689 – 701.

[12] a) R. R. Breaker, G. F. Joyce, *Chem. Biol.* **1994**, *1*, 223 – 229; b) S. K. Silverman, *Nucleic Acids Res.* **2005**, *33*, 6151 – 6163; c) K. Schlosser, Y. Li, *ChemBioChem* **2010**, *11*, 866 – 879.

[13] a) C. He, J. Bozler, K. A. Janssen, J. E. Wilusz, B. A. Garcia, A. J. Schorn, R. Bonasio, *Nat. Struct. Mol. Biol.* **2021**, *28*, 62 – 70; b) S. Haag, K. E. Sloan, N. Ranjan, A. S. Warda, J. Kretschmer, C. Blessing, B. Hubner, J. Seikowski, S. Dennerlein, P. Rehling, M. V. Rodnina, C. Höbartner, M. T. Bohnsack, *EMBO J.* **2016**, *35*, 2104 – 2119.

[14] a) C.-X. Song, C. Yi, C. He, *Nat. Biotechnol.* **2012**, *30*, 1107 – 1116; b) Y. Dai, B.-F. Yuan, Y.-Q. Feng, *RSC Chem. Biol.* **2021**, https://doi.org/10.1039/D1CB00022E.

[15] RNA labeling was performed with FH14 ribozyme: M. Ghaem Maghami, C. P. M. Scheitl, C. Höbartner, *J. Am. Chem. Soc.* **2019**, *141*, 19546 – 19549.

[16] a) I. Behm-Ansmant, M. Helm, Y. Motorin, *J. Nucleic Acids* **2011**, 408053; b) M. Heiss, S. Kellner, *RNA Biol.* **2017**, *14*, 1166 – 1174.

[17] T. Suzuki, Y. Yashiro, I. Kikuchi, Y. Ishigami, H. Saito, I. Matsuzawa, S. Okada, M. Mito, S. Iwasaki, D. Ma, X. Zhao, K. Asano, H. Lin, Y. Kirino, Y. Sakaguchi, T. Suzuki, *Nat. Commun.* **2020**, *11*, 4269.

[18] To facilitate access of the deoxyribozymes, disruptor oligonucleotides were included complementary to the 5′ or 3′ end of the acceptor stem, respectively (see D56 and D59 in the Supporting Information, Table S2).

[19] a) S. Kobori, Y. Yokobayashi, *Angew. Chem. Int. Ed.* **2016**, *55*, 10354 – 10357; *Angew. Chem.* **2016**, *128*, 10510 – 10513; b) V. Dhamodharan, S. Kobori, Y. Yokobayashi, *ACS Chem. Biol.* **2017**, *12*, 2940 – 2945; c) A. D. Pressman, Z. Liu, E. Janzen, C. Blanco, U. F. Müller, G. F. Joyce, R. Pascal, I. A. Chen, *J. Am. Chem. Soc.* **2019**, *141*, 6213 – 6223; d) J. O. L. Andreasson, A. Savinov, S. M. Block, W. J. Greenleaf, *Nat. Commun.* **2020**, *11*, 1663; e) Y. Yokobayashi, *Acc. Chem. Res.* **2020**, *53*, 2903 – 2912; f) Y. Shen, A. Pressman, E. Janzen, I. A. Chen, *Nucleic Acids Res.* **2021**, https://doi.org/10.1093/nar/gkab199.

Manuscript received: May 14, 2021
Revised manuscript received: June 20, 2021
Accepted manuscript online: June 29, 2021
Version of record online: July 26, 2021

